ELSEVIER

Thermochimica Acta 314 (1998) 307–315

thermochimica acta

Association in ternary metallic melts Fe–Mn–Si, Fe–Cr–P and Fe–Mn–P

A.I. Zaitsev*, A.D. Litvina, N.E. Shelkova, B.M. Mogutnov

Institute for Physical Metallurgy, I.P. Bardin Central Research Institute for Iron and Steel Industry, 9/23 2-nd Baumanskaya, Moscow 107005, Russia

Received 13 October 1997; accepted 5 January 1998

Abstract

Knudsen-cell mass-spectrometry was used to investigate the thermodynamic properties of liquid alloys Fe–Mn–Si (1435–1809 K), Fe–Cr–P (1403–1821 K) and Fe–Mn–P (1302–1701 K). Niobium or molybdenum double effusion cells with inner surfaces covered with ZrO_2 or Al_2O_3 were used in the experiments. Nickel, copper, chromium or strontium fluoride served as a reference substance. The saturated vapor was found to consist mainly of atoms Fe, Mn, Cr, Si, P and molecules P_2, Si_2. Representative files of data comprising 700, 1100, and 1500 values of activities of all components were received for the Fe–Mn–P, Fe–Cr–P and Fe–Mn–Si liquid solutions. The thermodynamic properties of the melts were approximated by the associated-solution model. For adequate representation of the experimental data it was necessary to take into account the binary associates, formed by iron, chromium and manganese atoms with silicon or phosphorus, ternary associative complexes FeMnSi, FeCrP or FeMnP and excessive terms describing interactions between monomer species. The thermodynamic characteristics of the binary associates were found to agree within the limits of experimental error with the values established earlier from the experimental data for binary systems. © 1998 Elsevier Science B.V.

Keywords: Thermodynamic properties; Fe–Mn–Si; Fe–Cr–P; Fe–Mn–P; Knudsen-cell mass spectrometry; Associated solutions; Ternary associates

1. Introduction

The thermodynamic properties of binary metallic solutions with strong inter-particle interactions dominated by covalent bonds are successfully approximated by models, founded on Prigogine's associated solution theory (see, e.g., [1,2]). However, it is not clear how this theory is to be applied to three and higher component systems of similar type. The authors of the most of the published works in the field (see, e.g., [3–5]) have considered only binary associates and attempted to extend it as in the case of the regular solutions, namely by introducing excess Gibbs energy terms which accounted for interactions between the binary associated-solution species. However, it seems more logical to consider possibility that ternary and higher-component associates might be formed. The alloys Fe–Mn–Si, Fe–Cr–P and Fe–Mn–P are convenient subjects for considerations of this kind, as the binary solutions of Si and P with Fe, Cr, or Mn are well described by the ideal associated-solution model [6–10] and the liquid mixtures of iron with manganese or chromium are close to the perfect solution and are characterized by only minor deviations from Raoult's law [11,12].

*Corresponding author.

PII S0040-6031(98)00265-2

2. Experimental

A Knudsen effusion technique combined with a mass-spectrometric analysis of the evaporated species was used in the present work to determine the thermodynamic properties of the Fe–Mn–Si, Fe–Cr–P, and Fe–Mn–P melts. The composition of samples and the temperature of experiments varied within the following ranges:

Fe–Mn–Si	Fe–Cr–P	Fe–Mn–P
$0 \le x_{Fe} \le 1$	$0.059 \le x_{Fe} \le 0.801$	$0.205 \le x_{Fe} \le 0.738$
$0 \le x_{Mn} \le 0.6$	$0.054 \le x_{Cr} \le 0.789$	$0.22 \le x_{Mn} \le 0.695$
$0 \le x_{Si} \le 1$	$0.048 \le x_{P} \le 0.318$	$0.152 \le x_{P} \le 0.365$
$1435 \le T \le 1823$	$1403 \le T \le 1821$	$1435 \le T \le 1823$

Samples of Fe–Mn–Si were melted in an argon-arc furnace with a water-cooled copper mold from iron of super-high purity (mass fraction $<10^{-6}$ of impurities), manganese of spectral purity (mass fraction $<10^{-5}$ of impurities) and semi-conductive silicon (mass fraction $<10^{-6}$ of impurities). The mass losses were negligible (<0.05 mass %) so that there was no need for chemical analysis of the molten products. Samples of Fe–Cr–P and Fe–Mn–P were prepared directly in the effusion cells from the same iron and manganese, electrolytic chromium (mass fraction $<10^{-4}$ of impurities) and binary Fe–P, Cr–P and Mn–P alloys, synthesized from the same metals and red phosphorus (99.995 mass %) as described in [6,7]. Random weighing, chemical and X-ray analyses of samples after subsequent experiments revealed that the chemical composition could be calculated with the necessary accuracy from the mass of the components.

Double effusion cells made from tantalum or niobium were used in experiments. The inner surfaces of the cells were covered with zirconia or alumina by plasma spraying in order to avoid chemical interaction between the samples and the cell materials. The orifice diameter varied from 0.2 to 0.42 mm while the effusion-cell diameter was 6 mm. Nickel, copper, chromium or SrF_2 were chosen as reference substances. Temperature functions of the ion currents (vapor pressures) of these substances were well reproducible in all cases and were in good agreement with the thermodynamic databank IVTANTERMO [13] and with data [14–17]. Reference substance data from the above sources were, therefore, used in vapor pressure calculations. Mass-spectra were obtained at energies of the ionising electrons equal to 5.6–8.9 J. The experimental procedure was the same as that reported earlier [15,16].

Lines corresponding to the molar masses 28, 55, and 56 g mol^{-1} were the main in the spectra of the saturated vapor over the Fe–Mn–Si solutions. The first two originated from Si^+ and Mn^+ formed by ionization of silicon and manganese atoms. The third could be caused by ions Fe^+ and Si_2^+ which have almost the same mass. The resolution of the mass-spectrometer was not enough to differentiate between the signals caused by these two ions. The Si_2^+ ion currents were calculated from the measured Si^+ line intensities and the equilibrium constant of the reaction $2Si(g) \leftrightarrow Si_2(g)$ as described previously [18]. Subtraction of the values found in this way from the intensities corresponding to the mass 56 line allowed us to determine the Fe^+ ion currents. The contribution of Si_2^+ to the total currents caused by ions of mass 56 g mol^{-1} was negligible in all cases except in samples of $x_{Si} \ge 0.63$, in which it did not exceed 10%. As in the study of the Fe–Si system [8], SiO^+ was also registered in the mass-spectra of saturated vapor over Fe–Mn–Si melts of high silicon content ($x_{Si} \ge 0.525$). These ions resulted from ionization of SiO molecules formed by reduction of the zirconia or alumina protective layers. The dependence of the SiO^+ ion current on the composition of the samples, the duration of the experiment, and the type of oxide coating was similar to that observed for the Fe–Si system [8]. In order to avoid any influence on intensities of Si^+ ion current of the fragmentary Si^+ ions which might appear through dissociative ionization of SiO molecules, only values of $I(Si^+)$ found in experiments having $I(SiO^+)/I(Si^+)$ ratios <0.10–0.12 were used for the vapor pressure calculations.

The major lines in the spectra of the saturated vapor over Fe–Cr–P and Fe–Mn–P corresponded to the ions of metals, P_2^+ and P^+. The conventional method based on the pressure independence of the equilibrium constants of some gaseous reactions, as well as previous results [6,7], were applied to assign the P^+ line. It was found that ions P^+ originated from P_2 molecules and P atoms. The concentration of P in the vapor increased, and that of P_2 decreased, with a reduction in phosphorus content in the samples and a rise in temperature. For instance, at 1811 K the concentration of P in the vapor above the Fe–Cr–P alloy with $x_P = 0.048$ and

x_{Cr}=0.151 was about 77% of that of P_2, while above the alloy with x_P=0.201 and x_{Cr}=0.300 the concentration of P was <1% of that of P_2 at all temperatures studied.

3. Results and discussion

Partial vapor pressures, activities, and partial thermodynamic functions of the components were calculated according to the well-known equations of the high-temperature mass-spectrometry, using the method reported in [6–9]. The results depended on neither the orifice diameter, nor the cell material and the type of coating on the inner surfaces of the cells. Equilibrium constants for the reaction $P_2(g) \leftrightarrow 2P(g)$, calculated from the measured vapor pressures of P_2 and P, agreed well with the values recommended by [13,19]. Activities of all three components were simultaneously determined for the most samples investigated. Rarely and mainly at low temperatures, the vapor pressures of only two or one component could be measured. As a result, representative files of data on the component activities at different compositions and/or temperatures comprising about 1500 values for Fe–Mn–Si, 1100 values for Fe–Cr–P, and 700 values for Fe–Mn–P melts were obtained. The activities are partly given in Table 1–3. Pure liquid com-

Table 1
Comparison of experimental component activities in the Fe–Mn–Si melt, chosen at random, with activities calculated with the associated-solution model (standard states: pure liquid components)

x_{Si}	x_{Mn}	T/K	a_{Mn}		a_{Si}		a_{Fe}	
			exp.	calc.	exp.	calc.	exp.	calc.
0.807	0.102	1808	0.00430	0.00433	0.769	0.770	0.00201	0.00197
0.807	0.102	1743	0.00353	0.00349	0.767	0.769	0.00152	0.00155
0.724	0.198	1743	0.00895	0.00901	0.645	0.639	0.00157	0.00160
0.724	0.198	1619	0.00575	0.00575	0.634	0.633	0.000944	0.000953
0.630	0.301	1640	0.0148	0.0145	0.454	0.453	0.00136	0.00135
0.630	0.301	1535	0.00983	0.00974	0.445	0.441	0.000843	0.000837
0.449	0.497	1528	0.0709	0.0716	0.0791	0.0780	0.00332	0.00332
0.365	0.600	1526	0.210	0.208	0.0169	0.0172	0.00579	0.00576
0.724	0.098	1804	0.00495	0.00501	0.631	0.626	0.00580	0.00571
0.724	0.098	1669	0.00308	0.00313	0.616	0.620	0.00345	0.00347
0.637	0.201	1665	0.00971	0.00982	0.456	0.454	0.00443	0.00437
0.556	0.304	1660	0.0242	0.0238	0.293	0.287	0.00570	0.00575
0.556	0.304	1493	0.0141	0.0139	0.252	0.255	0.00311	0.00306
0.474	0.405	1551	0.0480	0.0480	0.113	0.111	0.00723	0.00716
0.631	0.100	1792	0.00687	0.00687	0.439	0.436	0.0142	0.0139
0.631	0.100	1645	0.00424	0.00428	0.415	0.418	0.00866	0.00860
0.495	0.297	1622	0.0337	0.0333	0.154	0.153	0.0143	0.0145
0.495	0.297	1474	0.0229	0.0234	0.120	0.119	0.00976	0.00970
0.561	0.200	1630	0.0135	0.0136	0.280	0.276	0.0108	0.0107
0.568	0.051	1809	0.00468	0.00461	0.311	0.308	0.0306	0.0311
0.568	0.051	1612	0.00259	0.00261	0.269	0.269	0.0184	0.0183
0.512	0.149	1637	0.0135	0.0137	0.177	0.176	0.0247	0.0253
0.512	0.149	1469	0.00856	0.00849	0.140	0.138	0.0156	0.0159
0.450	0.251	1555	0.0363	0.0362	0.0719	0.0726	0.0309	0.0313
0.476	0.047	1761	0.00644	0.00645	0.152	0.150	0.0613	0.0608
0.476	0.047	1685	0.00557	0.00555	0.136	0.134	0.0529	0.0533
0.453	0.095	1721	0.0149	0.0151	0.110	0.110	0.0640	0.0634
0.379	0.053	1650	0.0141	0.0138	0.0377	0.0373	0.124	0.122
0.362	0.100	1635	0.0323	0.0316	0.0249	0.0254	0.137	0.135
0.287	0.045	1640	0.0290	0.0287	0.0062	0.00634	0.291	0.289

Table 2
Comparison of experimental component activities in the Fe–Cr–P melt, chosen at random, with activities calculated by the associated-solution model (standard states: pure liquid components)

x_P	x_{Cr}	T/K	a(P)		a(Cr)		a(Fe)	
			exp.	calc.	exp	calc.	exp.	calc.
0.103	0.102	1720	2.60×10^{-5}	2.56×10^{-5}	0.0762	0.0769	0.784	0.778
0.103	0.102	1791	3.93×10^{-5}	3.92×10^{-5}	0.0772	0.0776	0.769	0.778
0.103	0.102	1653	1.61×10^{-5}	1.64×10^{-5}	0.0759	0.0762	0.774	0.777
0.155	0.054	1596	2.91×10^{-5}	2.86×10^{-5}	0.0337	0.0334	0.713	0.716
0.155	0.054	1725	6.65×10^{-5}	6.73×10^{-5}	0.0338	0.0342	0.722	0.722
0.155	0.054	1817	1.11×10^{-4}	1.13×10^{-4}	0.0350	0.0346	0.723	0.726
0.048	0.151	1787	1.06×10^{-5}	1.08×10^{-5}	0.134	0.132	0.805	0.804
0.149	0.153	1503	1.11×10^{-5}	1.09×10^{-5}	0.0979	0.0985	0.648	0.648
0.149	0.153	1664	3.72×10^{-5}	3.68×10^{-5}	0.106	0.104	0.649	0.651
0.149	0.153	1809	8.71×10^{-5}	8.74×10^{-5}	0.110	0.108	0.658	0.655
0.175	0.226	1508	1.60×10^{-5}	1.62×10^{-5}	0.133	0.135	0.544	0.543
0.175	0.226	1659	4.91×10^{-5}	4.86×10^{-5}	0.144	0.145	0.549	0.547
0.201	0.300	1471	1.72×10^{-5}	1.74×10^{-5}	0.159	0.162	0.436	0.431
0.201	0.300	1630	5.51×10^{-5}	5.47×10^{-5}	0.179	0.180	0.439	0.441
0.201	0.300	1782	1.30×10^{-4}	1.31×10^{-4}	0.190	0.192	0.454	0.450
0.250	0.349	1517	5.90×10^{-5}	5.87×10^{-5}	0.160	0.158	0.293	0.295
0.250	0.349	1681	1.51×10^{-4}	1.52×10^{-4}	0.181	0.180	0.319	0.317
0.250	0.349	1809	2.87×10^{-4}	2.84×10^{-4}	0.192	0.192	0.334	0.329
0.302	0.397	1780	5.39×10^{-4}	5.37×10^{-4}	0.167	0.167	0.201	0.203
0.318	0.199	1704	1.00×10^{-3}	9.89×10^{-4}	0.0448	0.0444	0.240	0.240
0.202	0.500	1747	8.38×10^{-5}	8.31×10^{-5}	0.361	0.363	0.266	0.267
0.195	0.603	1765	7.33×10^{-5}	7.41×10^{-5}	0.476	0.476	0.178	0.176
0.146	0.705	1745	3.02×10^{-5}	2.99×10^{-5}	0.633	0.629	0.130	0.131
0.146	0.705	1814	4.42×10^{-5}	4.45×10^{-5}	0.642	0.641	0.131	0.131
0.143	0.798	1791	3.51×10^{-5}	3.55×10^{-5}	0.737	0.741	0.0475	0.0473
0.309	0.304	1755	7.12×10^{-4}	7.06×10^{-4}	0.0989	0.100	0.241	0.237
0.245	0.098	1603	1.55×10^{-4}	1.53×10^{-4}	0.0395	0.0393	0.446	0.449
0.245	0.098	1812	4.72×10^{-4}	4.67×10^{-4}	0.0427	0.0430	0.476	0.475

ponents were chosen as standard states. The Gibbs energies of phase transformations of manganese and silicon from the IVTANTERMO bank [13] and of phosphorus, iron and chromium from [19–21] were used to recalculate the thermodynamic functions with respect to these states.

In constructing the thermodynamic model, it was supposed that several types of ternary complexes Fe_kMnlSi_m, $Fe_kCr_lP_m$, and $Fe_kMn_lP_m$) could exist in the melt along with all binary associates, characteristic to the binary subsystems [6–10]: Fe–Si(FeSi, Fe_2Si, Fe_3Si, $FeSi_2$), Mn–Si(MnSi, Mn_2Si), Fe–P(FeP, Fe_2P, Fe_3P), Cr–P(CrP, Cr_2P, Cr_3P, Cr_3P_2), and Mn–P(MnP, Mn_2P, Mn_3P, Mn_3P_2). The mixing of Gibbs energy was expressed by the following equation:

$$\Delta_f G = \sum_i n_i \Delta_f G_i^0 + RT\left[\sum_i n_i \ln x_i + \sum_{J_l} n(J_1)\ln x(J_1)\right] + \Delta_f G^{ex} \quad (1)$$

$\Delta_f G_i^0 = -RT\ln K_i = \Delta_f H_i^0 - T\Delta_f S_i^0$ is the molar Gibbs energy of formation of i-type complex, K_i being the equilibrium constant of the reaction of its formation; n_i, x_i are the amounts of substance and mole fraction of i-type associative complex; $n(J_1)$ and $x(J_1)$ are the amount of substance and mole fraction of monomer species; $\Delta_f G^{ex}$ is the excess Gibbs energy change caused by interaction between the components of the associated solution. Summations are to be

Table 3
Comparison of experimental component activities in Fe–M*n*–P, chosen at random, with activities calculated with the associated-solution model (standard states: pure liquid components)

x_P	x_{Mn}	T/K	a_P		a_{Mn}		a_{Fe}	
			exp.	calc.	exp.	calc.	exp.	calc.
0.172	0.101	1354		5.46×10^{-6}	0.0779	0.0781	0.600	0.602
0.172	0.101	1430	1.15×10^{-5}	1.16×10^{-5}	0.07980	0.08030	0.6130	0.608
0.172	0.101	1462	1.58×10^{-5}	1.55×10^{-5}	0.08130	0.08130	0.6070	0.610
0.172	0.101	1524	2.54×10^{-5}	2.60×10^{-5}	0.08320	0.08310	0.6110	0.614
0.172	0.101	1558	3.37×10^{-5}	3.39×10^{-5}	0.08390	0.08400	0.6190	0.616
0.158	0.375	1384	6.41×10^{-6}	6.30×10^{-6}	0.25500	0.25500	0.4200	0.415
0.158	0.375	1443	1.09×10^{-5}	1.12×10^{-5}	0.26500	0.26600	0.4120	0.414
0.208	0.054	1391	1.60×10^{-5}	1.60×10^{-5}	0.04170	0.04130	0.5440	0.539
0.208	0.054	1470	3.16×10^{-5}	3.21×10^{-5}	0.04200	0.04230	0.5490	0.550
0.208	0.054	1543	5.74×10^{-5}	5.67×10^{-5}	0.04330	0.04310	0.5610	0.557
0.208	0.054	1602	8.62×10^{-5}	8.59×10^{-5}	0.04440	0.04380	0.5640	0.565
0.253	0.071	1517	1.32×10^{-4}	1.33×10^{-4}	0.04400	0.04390	0.3890	0.394
0.253	0.071	1576	2.00×10^{-4}	1.95×10^{-4}	0.04520	0.04550	0.4060	0.404
0.253	0.071	1598	2.25×10^{-4}	2.24×10^{-4}	0.46300	0.04600	0.4050	0.407
0.303	0.022	1634	1.19×10^{-3}	1.18×10^{-3}	0.00896	0.00896	0.2490	0.250
0.303	0.022	1678	1.39×10^{-3}	1.42×10^{-3}	0.00934	0.00937	0.2650	0.261
0.199	0.252	1390	1.47×10^{-5}	1.43×10^{-5}	0.15500	0.15800	0.4310	0.426
0.199	0.252	1438	2.21×10^{-5}	2.23×10^{-5}	0.16700	0.16400	0.4260	0.428
0.199	0.252	1464	2.84×10^{-5}	2.79×10^{-5}	0.16800	0.16800	0.4320	0.429
0.151	0.695	1302		1.56×10^{-6}	0.52200	0.5230	0.000	0.120
0.151	0.695	1409	5.42×10^{-6}	5.35×10^{-6}	0.541	0.54400	0.126	0.127
0.365	0.430	1540	2.65×10^{-3}	2.63×10^{-3}	0.0645	0.06440	0.0466	0.0471

carried out over all types of associative complexes and monomer species. In accordance with the conclusion in [22], the excess Gibbs energy was represented by the following series:

$$\Delta_f G^{ex} = \sum_{i,j,q} L_{ijq} \frac{n^i_{Fe} n^j_{Cr(Mn)} n^q_{Si(P)}}{(n_{Fe} + n_{Cr(Mn)} + n_{Si(P)})^{i+j+q-1}} \quad (2)$$

where n_{Fe}, $n_{Cr(Mn)}$ and $n_{Si(P)}$ are the amounts of substance of the components. Parameters L_{ijq} describe interactions between monomer species and are assumed to depend on temperature. Each subscript i, j, and q refers to the component of the solution Fe, Cr or Mn, Si or P and simultaneously indicates the order of interaction. For example, L_{111} characterizes the first-order interaction between all components and L_{202} – the second-order interaction between Fe and Si(P). The conventional procedure of deriving partial properties transforms the last relation into the set of equations for calculation of the activity coefficients of the associated solution species:

$$\ln\gamma(Fe_1) = \sum_{i,j,q} l_{ijq}\{i x^{i-1}_{Fe} x^j_{Cr(Mn)} x^q_{Si(P)} - (i+j+q-1) x^i_{Fe} x^j_{Cr(Mn)} x^q_{Si(P)}\} \quad (3)$$

$$\ln\gamma(Cr(Mn)_1) = \sum_{i,j,q} l_{ijq}\{j x^i_{Fe} x^{j-1}_{Cr(Mn)} x^q_{Si(P)} - (i+j+q-1) x^i_{Fe} x^j_{Cr(Mn)} x^q_{Si(P)}\} \quad (4)$$

$$\ln\gamma(Si(P)_1) = \sum_{i,j,q} l_{ijq}\{q x^i_{Fe} x^j_{Cr(Mn)} x^{q-1}_{Si(P)} - (i+j+q-1) x^i_{Fe} x^j_{Cr(Mn)} x^q_{Si(P)}\} \quad (5)$$

$$\gamma(Fe_k Cr(Mn)_1 Si(P)_m) = [\gamma(Fe_1)]^k [\gamma(Cr(Mn)_1)]^l [\gamma(Si(P)_1)]^m \quad (6)$$

where $l_{ijq}=L_{ijq}/RT$ Eq. (6) makes it possible to express the equilibrium constants of the complex formation

reactions in terms of the concentrations of the associated-solution species, i.e. in the form characteristic to the ideal-associated-solution model. This last result allows us to find concentrations of the monomer species in associated solution by solving the system of the equations connecting the mole fractions of the components with those of the associated-solution species. For the Fe–Mn–Si melt we obtain the following equations:

$$\begin{aligned} x(\mathrm{Fe}_1) = x(\mathrm{Fe}) &- \sum K(\mathrm{Fe_pSi_q})(x(\mathrm{Fe}_1))^p \\ &\times (x(\mathrm{Si}_1))^q[\mathrm{p} - x(\mathrm{Fe})(\mathrm{p}+\mathrm{q}-1)] \\ &- \sum \mathrm{K}(\mathrm{Fe_kMn_lSi_m})(x(\mathrm{Fe}_1))^k \\ &\times (x(\mathrm{Fe}_1))^k(x(\mathrm{Mn}_1)^1)(x(\mathrm{Si}_1))^m \\ &\times [k - x(\mathrm{Fe})(k+1+m-1)] \end{aligned} \quad (7)$$

$$\begin{aligned} x(\mathrm{Mn}_1) = x(\mathrm{Mn}) &- \sum K(\mathrm{Mn_pSi_q})(x(\mathrm{Mn}_1))^p \\ &\times (x(\mathrm{Si}_1))^q[\mathrm{p} - x(\mathrm{Mn})(\mathrm{p}+\mathrm{q}-1)] \\ &- \sum K(\mathrm{Fe_kMn_1Si_m})(x(\mathrm{Fe}_1))^k \\ &\times (x(\mathrm{Fe}_1))^k(x(\mathrm{Mn}_1)^1)(x(\mathrm{Si}_1))^m \\ &\times [l - x(\mathrm{Mn})(k+1+m-1)] \end{aligned} \quad (8)$$

$$\begin{aligned} x(\mathrm{Si}_1) = x(\mathrm{Si}) &- \sum K(\mathrm{Mn_pSi_q})(x(\mathrm{Mn}_1))^p \\ &\times (x(\mathrm{Si}_1))^q[\mathrm{q} - x(\mathrm{Si})(\mathrm{p}+\mathrm{q}-1] \\ &- \sum K(\mathrm{Fe_kMn_1Si_m})(x(\mathrm{Fe}_1)^k(x(\mathrm{Mn}_1)^l) \\ &\times (x(\mathrm{Si}_1))^m[m - x[(\mathrm{Si})(k+l+m-1)] \\ &- \sum K(\mathrm{Fe_pSi_q})(x(\mathrm{Fe}_1))^p(x(\mathrm{Si}_1)) \\ &\times \mathrm{q}[x(\mathrm{Si})(\mathrm{p}+\mathrm{q}-1)] \end{aligned} \quad (9)$$

Here $x(J_1)$ and $x(J)$ are mole fraction of the monomer species J_1 and overall mole fraction of component J. The component activities can be calculated by multiplying mole fractions of the monomer species by the corresponding activity coefficients from Eqs. (3)–(5).

To determine the types of ternary associative complexes and their thermodynamic characteristics, the complete files of the experimental data were treated with an optimizing procedure. This involved varying the model parameters, with the aim to find the values which minimized the sum-of-squares of discrepancies between the calculated and measured activities of the components. The simultaneous existence of up to five ternary associative complexes was considered, in which each index *k, l* or *m* altering in the range 1–3. The number of terms in the relation for $\Delta_f G^{ex}$ was varied in the range 1–7. At the first optimization stage, the thermodynamic parameters of all associates, including binary ones, were taken to be arbitrary. As a consequence, the thermodynamic functions of the binary complexes were found to coincide within the experimental errors with those established from the data for Fe–Si [8], Mn–Si [9], Fe–P [7], Cr–P [10], and Mn–P [6]. Some examples of the coincidence are given in Table 4.

For this reason, at the second stage of optimization the thermodynamic characteristics of the binary associative complexes were assumed to be equal to those obtained earlier [6–10] and only the thermodynamic parameters of ternary complexes and the coefficients in equation for $\Delta_f G^{ex}$ were varied. The computations revealed that the experimental data on the components activities can be described by the suggested model with a precision not worse than the experimental one (2–3%), if only one ternary complex FeMnSi, FeCrP,

Table 4
Comparison of the thermodynamic characteristics of some binary associates, found as a result of optimising the experimental data for the ternary systems, with values, obtained from the data for binary melts

Composition of an associate	Present results		Found from binary systems	
	$-\Delta_f H_i^0$/J mol^{-1}	$-\Delta_f S_i^0$/J mol^{-1} K^{-1}	$-\Delta_f H_i^0$/J mol^{-1}	$-\Delta_f S_i^0$/J mol^{-1} K^{-1}
FeP[a]	81540	1.7	81025	1.4
FeP[b]	80690	1.2	81025	1.4
Mn_2P	174300	36.6	175252	37.2
Cr_2P	230020	53.8	229587	53.6
FeSi	100285	24.1	99814	23.8
Mn_2Si	98917	13.82	99300	14.10

[a] Calculated from data for the Fe–Mn–P melt.
[b] Calculated from data for the Fe–Cr–P melt.

or FeMnP and two or three terms in Eq. (2) were taken into account. The following values were found to be optimal:

Fe–Mn–Si

$$\Delta_f H^0(\mathrm{FeMnSi}) = -105509\,\mathrm{J\,mol^{-1}},$$
$$\Delta_f S^0(\mathrm{FeMnSi}) = -15.31\,\mathrm{J\,mol^{-1}K^{-1}}$$

$$L_{110} = -1525\,\mathrm{J\,mol^{-1}},$$
$$L_{120} = -28900 + 15.42T\,\mathrm{J\,mol^{-1}},$$
$$L_{111} = -31715\,\mathrm{J\,mol^{-1}}$$

Fe–Mn–P

$$\Delta_f H^0(\mathrm{FeMnP}) = -1622300\,\mathrm{J\,mol^{-1}},$$
$$\Delta_f S^0(\mathrm{FeMnP}) = -27.1\,\mathrm{J\,mol^{-1}K^{-1}}$$

$$L_{110} = -1604\,\mathrm{J\,mol^{-1}},$$
$$L_{120} = -32300 + 17.74T\,\mathrm{J\,mol^{-1}},$$
$$L_{111} = -26290\,\mathrm{J\,mol^{-1}}$$

Fe–Cr–P

$$\Delta_f H^0(\mathrm{FeCrP}) = -150060\,\mathrm{J\,mol^{-1}},$$
$$\Delta_f S^0(\mathrm{FeCrP}) = -25.1\,\mathrm{J\,mol^{-1}K^{-1}}$$

$$L_{110} = -970\,\mathrm{J\,mol^{-1}},$$
$$L_{111} = -79830\,\mathrm{J\,mol^{-1}}$$

In practice, these values were independent of whether the thermodynamic properties [6–10] of the binary-associated complexes were used in the optimization procedure or determined exclusively from the experimental data on ternary melts. The adequacy of the model is illustrated by the data in Tables 1–3.

In essence, the ternary complexes found are the simplest of all possible ternary associates. They can be treated as additive combinations of the two binary associates Fe_2–Si and Mn_2–Si, Fe_2–P and Cr_2–P or Fe_2–P and Mn_2–P. It is important that the enthalpies and entropies of formation of the ternary complexes are close to the average over the enthalpies and entropies of formation of the mentioned binary associates. This seems quite logical because the energetic parameters of formation Fe–Si and Mn–Si [8,9], Fe–P and Cr–P [7,10], Fe–P, and Mn–P [6,7] are close to each other. It opens up the possibilities of predicting the thermodynamic characteristics of ternary solutions from the properties of their binary constituents.

The coefficients L_{110} and L_{120}, found from the data for Fe–Mn–Si and Fe–Mn–P liquid solutions, describe the thermodynamic properties of the Fe–Mn melt. Note that the values of these coefficients computed from the data on both ternary systems agree well. They show that the liquid alloys of iron with manganese are characterized by minor negative deviations from ideality which practically coincide with those established in the latest and probably most careful investigation of Jacob et al. [11]. The computation of the lines of the equilibrium between the melt and the fcc phase of the Fe–Mn system was carried out, using the chemical equipotential approach, the present thermodynamic functions and the functions of the solid solution established earlier [23,24]. The Gibbs energies of the phase transformations of manganese and iron were taken from the IVTANTERMO bank [13] and data of Chuang et al.[20]. The results of computation are compared in Fig. 1 with the co-ordinates recommended in Kubaschewski's reference-book [25] and experimental data [26]. As one can see, there is an excellent agreement between the results of the calculations and the data of the independent sources listed.

The coefficient L_{110} describes the thermodynamic properties of the Fe–Cr melt. It shows that the liquid Fe–Cr alloys are characterized by minor negative deviation from Raoult's law which practically coincide with the data of Mills and Grieveson [12] obtained in high-temperature (2000–2200 K) experiments. Computation of the lines of equilibrium between the melt and bcc phase of the Fe–Cr system was carried out, using the same approach, the present thermodynamic functions of the liquid solution, the functions of the bcc solid solution established in our previous investigations [17,23,27], and the Gibbs energies of the phase transformations of iron and chromium recommended in [20,21]. The results of the computation are compared in Fig. 2 with the co-ordinates of (α+l) [25] and with experimental data [26,28–31]. As one can see, there is excellent agreement between the results of the calculations and the data of the independent sources listed in the low temperature region. In the high-temperature region (high concentrations of chromium) the calculated solids and liquids lines are situated somewhat higher. This slight disagreement can be explained by the differences in the temperature scales. Note that the authors [28] accepted for the melting temperatures of iron and chromium the values 1801 and 2103 K, respectively, whereas in the present study the up-to-date fusion temperatures 1809 and 2130 K [20,21] were used.

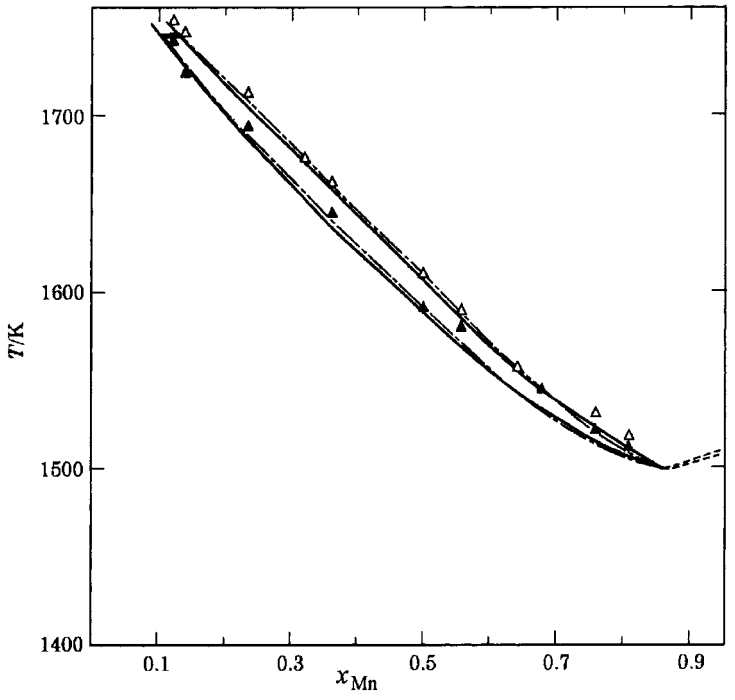

Fig. 1. Lines of l+fcc–solid solution equilibrium in the Fe–Mn system. (———) – present results; (–···–···) reference book [25]; Δ and ▲ – data [26].

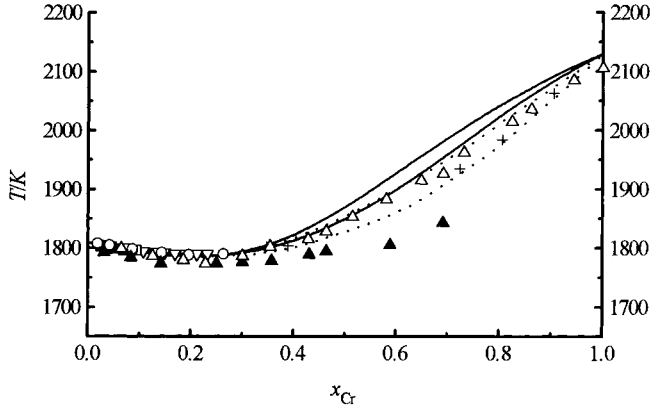

Fig. 2. Lines of equilibrium l+bcc–solid solution in the Fe–Cr system. (———), results of the present computation;(- - -), reference book [25]; experimental data: Δ – liquidus and ▲ – solidus lines [28], ○ – liquidus and ● – solidus lines [26], □ – liquidus and ■ – solidus lines [29], ∇ – liquidus line [30], + liquidus line [31].

References

[1] F. Sommer, Z. Metallkd. 73 (1982) 72.
[2] A.G. Morachevskii, E.A. Maiorova, in: Physico-Chemical Studies of Metallurgical Processes, UPI Publ., Sverdlovsk, 1980, p. 35.
[3] A. Launger, Rev. Phys. Appl. 8 (1973) 351.
[4] I. Arpshoven, M.J. Pool, F. Sommer, U. Gerling, B. Predel, E. Schultheiss, Z. Metallkd. 74 (1983) 25.
[5] Y.Y. Chuang, Y.A. Chang, Metall. Trans. 13B (1982) 379.
[6] A.I. Zaitsev, M.A. Zemchenko, A.D. Litvina, B.M. Mogutnov, Z. Metallkd. 84 (1993) 178.

[7] A.I. Zaitsev, Zh.V. Dobrokhotova, A.D. Litvina, B.M. Mogutnov, J. Chem. Soc., Faraday Trans. 95 (1995) 703.
[8] A.I. Zaitsev, M.A. Zemchenko, B.M. Mogutnov, J. Chem. Thermodyn. 23 (1991) 831.
[9] A.I. Zaitsev, M.A. Zemchenko, B.M. Mogutnov, Rasplavy 2 (1989) 9.
[10] A.I. Zaitsev, Zh.V. Dobrokhotova, A.D. Litvina, N.E. Shelkova, M.B Mogutnov, Inorg. Materials 32 (1996) 534.
[11] K.T. Jacob, J.P. Hajra, M. Iwase, Arch. Eisenhüttenwes. 55 (1984) 421.
[12] K.S. Mills, P.P. Grieveson, J. Chem. Thermodyn. 8 (1976) 545.
[13] L.V. Gurvich, Vestnik Akad. Nauk SSSR 3 (1983) 54.
[14] A.I. Zaitsev, M.A. Zemchenko, B.M. Mogutnov, Zh. Fiz. Khim. 64 (1990) 3377.
[15] A.I. Zaitsev, N.V. Korolyov, B.M. Mogutnov, Teplophys. Visokikh Temperatur 27 (1989) 465.
[16] A.I. Zaitsev, N.V. Korolyov, B.M. Mogutnov, High Temp. Sci. 28 (1990) 341.
[17] A.I. Zaitsev, M.A. Zemchenko, B.M. Mogutnov, Zh. Fiz. Khim. 64 (1990) 1187.
[18] A.I. Zaitsev, M.A. Zemchenko, B.M. Mogutnov, Zh. Fiz. Khim. 64 (1990) 1930.
[19] I. Karakaya, W.T. Tompson, Bull. Alloy Phase Diagrams 9 (1988) 232.
[20] Y.Y. Chuang, R. Schmid, Y.A. Chang, Metall. Trans. 16A (1985) 153.
[21] R. Hultgren, P.D. Desai, D.T. Hawkins, M. Gleiser, K.K. Kelley, D.W. Wagmann, Selected Values of the Thermodynamic Properties of the Elements, Metals Park, Ohio, 1973, p. 134.
[22] A.I. Zaitsev, N.V. Korolyov, B.M. Mogutnov, J. Chem. Thermodyn. 22 (1990) 531.
[23] A.I. Zaitsev, M.A. Zemchenko, B.M. Mogutnov, High Temp. Sci. 28 (1990) 313.
[24] A.I. Zaitsev, M.A. Zemchenko, B.M. Mogutnov, Zh. Fiz. Khim. 63 (1989) 2051.
[25] O. Kubaschewski, Iron Binary Phase Diagram, Springer, Berlin, 1982.
[26] A. Hellawell, W. Hume-Rothery, Philos. Trans. Roy. Soc. London 249 (1957) 417.
[27] A.I. Zaitsev, M.A. Zemchenko, B. M Mogutnov, Zh. Fiz. Khim. 64 (1990) 1195.
[28] F. Adcock, J. Iron Steel Institute 124 (1931) 99.
[29] E. Schurmann, J. Brauckmann, Arch. Eisenhüttenwes. 48 (1977) 3.
[30] D.M. Kundrat, M. Chochol, J.F. Elliott, Metall. Trans. 15B (1984) 663.
[31] J.W. Putman, R.D. Potter, M.J. Grant, Trans. ASM 43 (1951) 824.